Synthesis and Processing of Ultra-High Temperature Metal Carbide and Metal Diboride Nanocomposite Materials

Final Performance Report

Contract Number: FA9550-04-1-0140

Submitted to:

Dr. Joan Fuller

Program Manager

High Temperature Aerospace Materials Directorate of Aerospace, Chemistry and Material Sciences

Air Force Office of Scientific Research

By:

Robert F. Speyer

Professor

School of Materials Science and Engineering

Georgia Institute of Technology

771 Ferst Drive

Atlanta, GA 30332-0245

Robert.Speyer@mse.gatech.edu

REPORT DOCUMENTATION PAGE	*Form Approved* *OMB No. 0704-0188*

1. REPORT DATE *(DD-MM-YYYY)*	2. REPORT TYPE	3. DATES COVERED *(From - To)*
15-04-2008	Final Performance Report	1/05-12/07

4. TITLE AND SUBTITLE
Synthesis and Processing of Ultra-High Temperature Metal Carbide And metal Diboride Nanocomposite Materials

5a. CONTRACT NUMBER
FA9550-04-1-0140

5b. GRANT NUMBER

5c. PROGRAM ELEMENT NUMBER

6. AUTHOR(S)
Robert F. Speyer

5d. PROJECT NUMBER

5e. TASK NUMBER

5f. WORK UNIT NUMBER

7. PERFORMING ORGANIZATION NAME(S) AND ADDRESS(ES)
School of Materials Science and Engineering
Georgia Institute of Technology
771 Ferst Drive
Atlanta, GA 30332-0245

8. PERFORMING ORGANIZATION REPORT NUMBER

9. SPONSORING/MONITORING AGENCY NAME(S) AND ADDRESS(ES)
Air Force Office of Scientific Research
High Temperature Aerospace Materials Directorate of Aerospace, Chemistry and Materials Sciences
875 North Randolph Street, Suite 325, Rm 3112
Arlington , VA 22203

10. SPONSOR/MONITOR'S ACRONYM(S)

11. SPONSOR/MONITOR'S REPORT NUMBER(S)

12. DISTRIBUTION/AVAILABILITY STATEMENT
No limitations

13. SUPPLEMENTARY NOTES

14. ABSTRACT
Zirconium diboride and a zirconium diboride/tantalum diboride mixture were synthesized by solution-based processing. Zirconium n-propoxide was refluxed with 2,4-pentanedione to form zirconium diketonate. This compound hydrolyzed in a controllable fashion to form a zirconia precursor. Spherical particles of 200-600 nm for pure ZrB2 and ZrB2-TaB2 mixtures were formed. Commercial powders of ZrB2 containing various concentrations of B4C, SiC, TaB2, and TaSi2 were pressureless-sintered and post-HIPed to their theoretical densities. Oxidation resistances were studied by scanning thermogravimetry over the range 1150-1550°C. SiC additions improved oxidation resistance over a broadening range of temperatures with increasing SiC content. Tantalum additions to ZrB2-B4C-SiC in the form of TaB2 and/or TaSi2 increased oxidation resistance over the entire evaluated spectrum of temperatures. TaSi2 proved to be a more effective additive than TaB2. Silicon-containing compositions formed a glassy surface layer, covering an interior oxide layer. This interior layer was less porous in tantalum-containing compositions.

15. SUBJECT TERMS
Zirconium Diboride, Synthesis, Oxidation Resistance

16. SECURITY CLASSIFICATION OF: a. REPORT	b. ABSTRACT	c. THIS PAGE	17. LIMITATION OF ABSTRACT	18. NUMBER OF PAGES	19a. NAME OF RESPONSIBLE PERSON
					Robert F. Speyer
U	U	U	UU	17	**19b. TELEPHONE NUMBER** *(Include area code)* (404) 894-6075

Reset

I Executive Summary

This research was originally funded based on a proposal by Professor Michael Sacks (School of Materials Science and Engineering, Georgia Tech) which focused on the fabrication of highly sinterable and intimately-mixed zirconium diboride-based composite powders. The student working on this project was Ms. Yanli Xie (Ph.D. candidate, graduation Spring 2008). Upon Dr. Sack's departure in 2005, the contract was taken over by Professor Robert Speyer who advised Ms. Xie on the original work, and also employed Mr. Fei Peng (Ph.D. candidate, graduation Summer 2008). Mr. Peng's work focused on oxidation resistance of these multiphase systems based on sintered commercially-available powders. Each project is summarized below:

Synthesis: Zirconium diboride and a zirconium diboride/tantalum diboride mixture were synthesized by solution-based processing. Zirconium n-propoxide was refluxed with 2,4-pentanedione to form zirconium diketonate. This compound hydrolyzed in a controllable fashion to form a zirconia precursor. Boria and carbon precursors were formed via solution additions of phenol-formaldehyde and boric acid, respectively. Tantalum oxide precursors were formed similarly as zirconia precursors, in which tantalum ethoxide was used. Solutions were concentrated, dried, pyrolyzed (800-1100°C, 2 h, flowing Ar), and exposed to carbothermal reduction heat-treatments (1150-1800°C, 2h, flowing Ar). Spherical particles of 200-600 nm for pure ZrB_2 and ZrB_2-TaB_2 mixtures were formed (Publication: Y. Xie, T. H. Sanders, Jr., and R. F. Speyer, "Solution-based Synthesis and Processing of Sub-micron ZrB_2 and ZrB_2-TaB_2," in press, *J. Am. Ceram. Soc.*, April 2008).

Single-phase ZrB_2 powders were prepared with initial compositions of C/Zr = 4.8 and B/Zr = 3.0. ZrB_2-based composite powders with ZrC, ZrO_2, TaB_2, TaC, SiC, $TaSi_2$ and B_4C were prepared with particle sizes of 10-500 nm. The relative densities of ZrB_2/B_4C, ZrB_2/TaB_2, $ZrB_2/TaB_2/B_4C$, and $ZrB_2/TaSi_2$ were in the range of 91%-97% after pressureless sintering at 2020°C for 1 h or 30 min (Thesis: Y. Xie, Georgia Tech, Spring 2008).

Oxidation Resistance: Specimens of ZrB_2 containing various concentrations of B_4C, SiC, TaB_2, and $TaSi_2$ were pressureless-sintered and post-HIPed to their theoretical densities. Oxidation resistances were studied by scanning thermogravimetry over the range 1150-1550°C. SiC additions improved oxidation resistance over a broadening range of temperatures with increasing SiC content. Tantalum additions to ZrB_2-B_4C-SiC in the form of TaB_2 and/or $TaSi_2$ increased oxidation resistance over the entire evaluated spectrum of temperatures. $TaSi_2$ proved to be a more effective additive than TaB_2. Silicon-containing compositions formed a glassy surface layer, covering an interior oxide layer. This interior layer was less porous in tantalum-containing compositions. (Publication: F. Peng and R. F. Speyer, "Oxidation Resistance of Fully Dense ZrB_2 with SiC, TaB_2, and $TaSi_2$ Additives," in press, *J. Am. Ceram. Soc.*, April 2008).

II Background

Transition metal borides, specifically ZrB_2 and HfB_2 are of interest for aerospace applications because of their ultra-high melting temperature (>3000°C), high hardness and strength, and high thermal and electrical conductivities [1]-[3]. They are candidates for high-speed aircraft leading edges, as well as for structural parts in high temperature environments. Engineering of these ceramics for these applications has focused on formation of highly-sinterable powders and sintering aid additions to facilitate pressureless sintering of near-net-shape parts, and incorporation of additives which increase oxidation resistance through the formation of a passive amorphous oxide surface coating.

II.1 Synthesis

Metal borides can be synthesized by reaction between a metal oxide and boron oxide via a carbothermal reduction [4, 5]: $MO_{2(s)} + B_2O_{3(s)} + 5C_{(s)} \rightarrow MB_{2(s)} + 5CO_{(g)}$. Excess boria is generally required for the above reaction because of B_2O_3 volatilization at elevated temperatures (boiling point of B_2O_3, i.e. 1 atm vapor pressure, is 1860°C [6]). Homogeneous products with fine particle size have been reported [6]-[8] using this fabrication route. Metal carbides have been observed as intermediate reaction products during metal diboride synthesis because of preferential carbothermal reduction of the metal oxide by carbon. However, the metal diboride is formed eventually if sufficient boron is available, i.e., $MC_{(s)} + B_2O_{3(s)} + 2C_{(s)} \rightarrow MB_{2(s)} + 3CO_{(g)}$.

Chemical solution processing routes refer to methods in which one or all of the components (i.e., metal-bearing, boron-bearing and carbon-bearing) are solubilized in a liquid processing medium. Soluble sources that are used to provide boron including boric acid and boron alkoxides. Numerous soluble carbon-bearing materials have been used to produce metal carbides, including phenolic resins, furfuryl alcohol, sugar, corn starch, petroleum pitch, polyacrylonitrile (PAN) polymers, cellulose acetate polymers, and diols. Common soluble metal/metal oxide-bearing materials are metal alkoxides, metal diketonates, and metal carboxylates. Metal-organic compounds are usually subjected to hydrolysis and condensation reactions to produce polymeric or colloidal metal-oxide precursors [9]-[25]. Depending on the reaction conditions, the metal-organic compound may also be a source for some of the carbon for the carbothermal reduction reaction.

The most important advantage of solution-processing methods is that more intimate mixing of components (atomic-scale or at least molecular-scale mixing) can be achieved. However, it should be noted that preparation of solutions with atomic- or molecular-scale mixing does not necessarily ensure that the same scale of mixing will be maintained during subsequent processing steps. It is necessary to remove the liquid medium in a manner that avoids segregation of components. For example, molecular-scale mixing in the solutions may be maintained by first gelling the solutions prior to solvent removal. The hydrolysis time, temperature, and atmosphere can be altered to control the grain size and phase distribution in the resulting product, which in turn will factor into the properties of the resulting materials [26]-[28].

II.2 Densification

Historically, ZrB_2 and HfB_2 have been hot-pressed in order to achieve high relative densities—required for improved strength and thermal conductivity, and so that porosity does not mitigate oxidation resistance. Gash et al. hot pressed HfB_2-20 vol% SiC at 2200°C for 1 h to theoretical density [29]. More recently, pressureless sintering methods have been developed to achieve high relative densities. Sciti et al. found that a ZrB_2-$MoSi_2$ powder mixture sintered well, likely via a liquid-phase sintering mechanism, and the silicon constituent facilitated improved oxidation resistance similar to the silicon from SiC additions [30] (discussed shortly). Fahrenholtz et al. have shown that high relative density can be achieved from pressureless sintering of zirconium diboride if boron oxide particle coatings are removed by vacuum heat-treatment prior to the onset of sintering, and via the use of boron carbide additives which react with ZrO_2 impurities (to form ZrB_2, $CO_{(g)}$ and volatile $B_2O_{3(l)}$) which would otherwise hinder sintering [31, 32]. In other work, they found that WC additions (introduced via milling), and a more patient sintering period (540 min at 2150°C) also resulted in high relative density (∼98%) [33].

II.3 Oxidation Resistance

ZrB_2 exposed to air at elevated temperatures reacts with oxygen to form ZrO_2 and B_2O_3. The B_2O_3 scale is non-protective since boria has a high vapor pressure above ∼1200°C (boiling point, i.e. 1 atm vapor pressure, is 1860°C). For ZrB_2 + 20 vol% SiC, oxidation heat treatments at 1200°C and below showed weight gain no less extensive than those of specimens composed of ZrB_2 alone. However, above 1200°C, a borosilicate coating forms which has proven to be more impermeable to atmospheric oxygen penetration [34, 35]. Given the high volatility of boron oxide, the silica content of the borosilicate glass surface coating would be expected to increase with increasing temperature. However, the B_2O_3 vapor pressure may be suppressed by B_2O_3 entering into solution with SiO_2. Compositional analysis has shown that the boron content of the oxide layer after heating to 1500°C for 30 min was less than 1 wt% [36].

Opila et al. showed that a ZrB_2-20 vol% SiC composition exposed to 10 min oxidation cycles (repeated 10×) at 1327 and 1627°C developed protective oxide scales: 30 μm at 1327°C and 150 μm at 1627°C [37]. Thermal cycling at 1927°C resulted in an oxide layer thickness of over 1 mm. The 1627°C surface oxide coating was identified (via energy dispersive spectroscopy) to be silica. Underneath this coating was a region of ZrO_2 dispersed in silica, which in turn was above a region of ZrB_2 depleted of SiC. This last region was argued to have resulted from active oxidation of SiC to form $SiO_{(g)}$ [38, 37]. Opeka et al. have suggested that formation of $SiO_{(g)}$ could build up to pressures exceeding ambient, facilitating rupture of the protective glass layer, resulting in a cyclic protective/non-protective scale-forming sequence [39]. At 1927°C, active oxidation of SiC to form $SiO_{(g)}$ implies that no protective silicate liquid surface layer forms.

Talmy et al. investigated additions of Cr-, Ti-, Nb-, V-, and Ta-borides to ZrB_2 - 25 vol%

SiC, and found that all additions (all of which formed solid solutions with ZrB_2 after sintering) improved cyclic oxidation resistance over the base composition, with TaB_2 additions being the most effective [40]. It was found that improved oxidation resistance correlated with increasing cation field strength (defined as Z/r^2, where Z is the valence of the cation and r is the ionic radius) of the added diborides. In a borosilicate or silicate glass with transition metal cations, the tendency toward liquid immiscibility is known to increase with increasing cation field strength of the transition metal. This phase separation has been argued to result in increased viscosity [41], which has been correlated to reduced oxygen diffusion rates [39].

Opila et al. found that a ZrB_2-20 vol% SiC-20 vol% $TaSi_2$ composition showed a lower oxidation rate after cyclic oxidation at 1627°C than a ZrB_2-20 vol% SiC composition, or a HfB_2-20 vol% SiC-20 vol% SiC composition [42]. Improved oxidation resistance was related to evidence of phase separation in the amorphous surface layer. Talmy et al. demonstrated the presence of phase separation in a ZrB_2-2 vol% Ta_5Si_3 system based on a periodic pattern of glassy and crystalline areas on the oxidized surface [43]. In Opila et al.'s work, the composition containing $TaSi_2$ showed rapid consumption as compared to ZrB_2-20 vol% SiC compositions exposed to similar oxidation heat treatments at 1927°C. This was attributed to melting of Ta_2O_5 (1785°C) and/or compounds of Ta_2O_5 and ZrO_2. A purported advantage of tantalum compound additions is that the tantalum impurity can stabilize zirconium oxide, circumventing the tetragonal/monoclinic phase transformation (whose volume contraction upon cooling can create fissures in the oxide scale), and potentially reduce oxygen transport through what is normally a fast anion conductor [44]. Zhang et al. added 10 vol% LaB_6 to a ZrB_2-SiC-based UHTC and found substantial enhancement of oxidation resistance at 2400°C [45] (via an oxyacetylene torch; likely a low oxygen partial pressure environment). This was attributed to stabilization of the cubic ZrO_2 oxidation product, and the formation of low ionic mobility $La_2Zr_2O_7$ which has a melting temperature above 2300°C.

III Important Research Results

III.1 Synthesis of Sub-micron ZrB_2 and ZrB_2-TaB_2 Powder Mixtures

III.1.1 Synthesis Methodology

A flow chart for the solution-based synthesis of ZrB_2 is shown in Figure 1. The starting

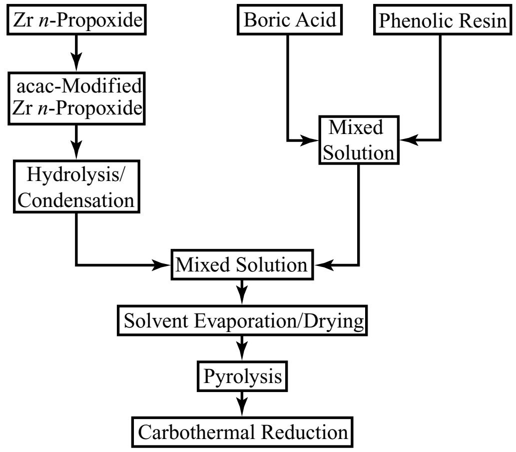

Figure 1: Flow chart for synthesis of ZrB_2 from solution-based precursors.

Zr-containing material was a 70 wt% zirconium n-propoxide ($Zr(OC_3H_7)_4$, Alfa Aesar, Ward Hill, MA) in solution with n-propanol. The zirconium n-propoxide ("$Zr(OPr)_4$") was mixed with 2,4-pentanedione ("acacH") using molar ratios of 3 (acacH to $Zr(OPr)_4$) and 2-propanol was used as a mutual diluent. This solution was refluxed (i.e. solution was heated and the vapor formed was condensed and returned to the solution to be heated again) at 170-195°C for 2 h for the purpose of reacting zirconium n-propoxide and 2,4-pentanedione to form zirconium diketonate, as illustrated in Figure 2. The purpose of this was to facilitate

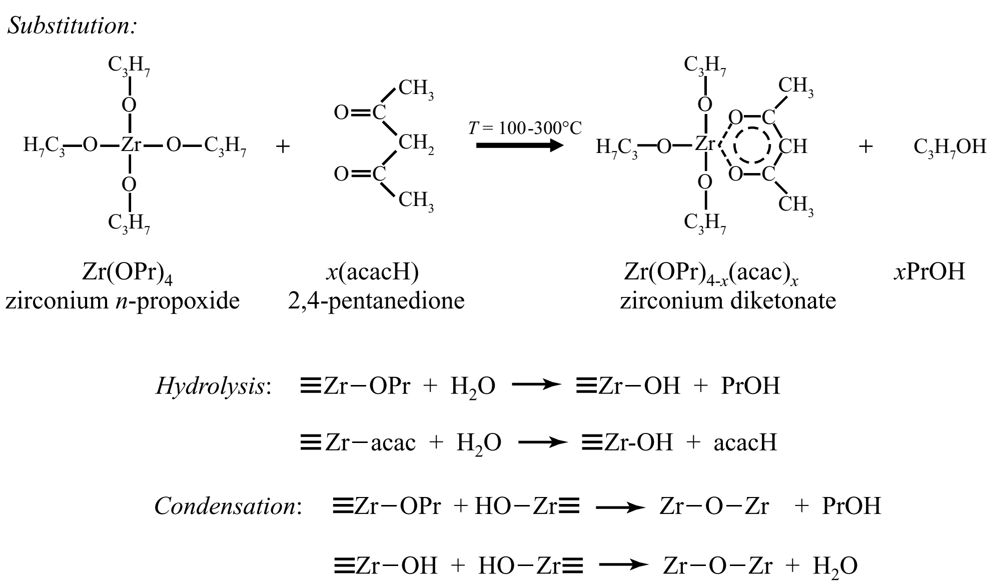

Figure 2: Reactions for precursor synthesis.

a controlled hydrolysis reaction; zirconium n-propoxide otherwise hydrolyzes very rapidly.

Refluxing maintains constant concentrations of constituents as reactions occur among them at temperatures at which their volatilities vary substantially. Following refluxing, much of the solvent (about 2/3) was evaporated using a rotary evaporator (Rotavapor R-114, BUCHI, Switzerland) at 35°C, and then 2-propanol was added back to the sol; the purpose of this was to remove remaining 2,4-pentanedione from the solution. These Zr-containing precursors were then partially hydrolyzed, in which a hydroxyl substituted for the *n*-propoxide and pentanedionate (acac) by interaction with water at 50°C for 2 h under acidic conditions (pH in the range 4-5) using a HNO_3/Zr molar ratio of 0.27 and an H_2O/Zr molar ratio of 24. Hydrolysis is required to facilitate later condensation reactions. A clear solution was observed before and after hydrolysis.

Separately, a boric acid (H_3BO_3, Fisher Scientific, Fair Lawn, NJ) in water solution with a concentration of 4 wt% was prepared as the boron source, to make a B/Zr ratio of 3. 2-propanol was then added to dilute the boric acid solution with a propanol/H_2O ratio of 3. 20 wt% phenol-formaldehyde resin (novolac-type, Georgia Pacific, Atlanta, GA) in a 2-propanol solution was added to the boric acid solution to increase the C/Zr ratio to 4.8-6.0.

The mixture of boric acid and phenol-formaldehyde resin was then added to the hydrolyzed Zr-containing solutions. The solutions were concentrated in a rotary evaporator (preventing the constituents from de-mixing) in a condensation reaction in which there is a buildup of species with a 3-dimensional structure. As solvent was volatilized, a residual mass formed with a sludge-like consistency. This was then dried to powders under vacuum conditions at 120-140°C (2 h). These powders were subsequently pyrolyzed at temperatures in the range of 800-1100°C (2 h) in a flowing argon atmosphere in an alumina tube-furnace to produce intimately-mixed not-yet-reacted zirconia/boron oxide/carbon mixtures. This temperature range was found to permit near-complete conversion to the desired oxide or carbon constituents, but was not high enough to initiate carbothermal reduction. Pyrolyzed powders were subsequently heat treated at temperatures in the range of 1200-1400°C (2 h) in flowing argon in a graphite tube-furnace for carbothermal reduction.

III.1.2 Zirconium Diboride

In general, zirconium *n*-propoxide undergoes more rapid hydrolysis reactions than the corresponding zirconium pentanedionate, and this has resulted in uncontrolled precipitation of relatively large precursor particles during the hydrolysis step. Therefore, zirconium n-propoxide was first refluxed (195°C, 2 h) with 2,4 pentanedione in order to partially or fully convert the zirconium alkoxy groups to a chelated zirconium diketonate structure.

An idealized reaction to produce stoichiometric ZrB_2 by carbothermal reduction is given by:

$$ZrO_{2(s)} + B_2O_{3(s)} + 5C_{(s)} \rightarrow ZrB_{2(s)} + 5CO_{(s)}$$

However, the necessary ratio of boron to zirconium was found to be ∼3:1 instead of 2:1 as dictated by reaction stoichiometry. Excess boron oxide was required to form ZrB_2 because of B_2O_3 volatilization at elevated temperatures.

The as-dried precursor was XRD-amorphous. Initial formation of ZrB_2 was observed after heat-treatment at 1200°C, while the intensity of t-ZrO_2 increased compared with m-ZrO_2 in the range 1100-1250°C. Zirconia phases reduced to minor levels at 1300°C, and were not observed at 1400°C. Weight loss measurements imply that the carbothermal reduction proceeded extensively above 1100°C, and tapers-off after heat-treatments at 1300°C. Figure 3 shows an SEM photomicrograph of a sample (initial composition was C/Zr = 5.0, B/Zr =

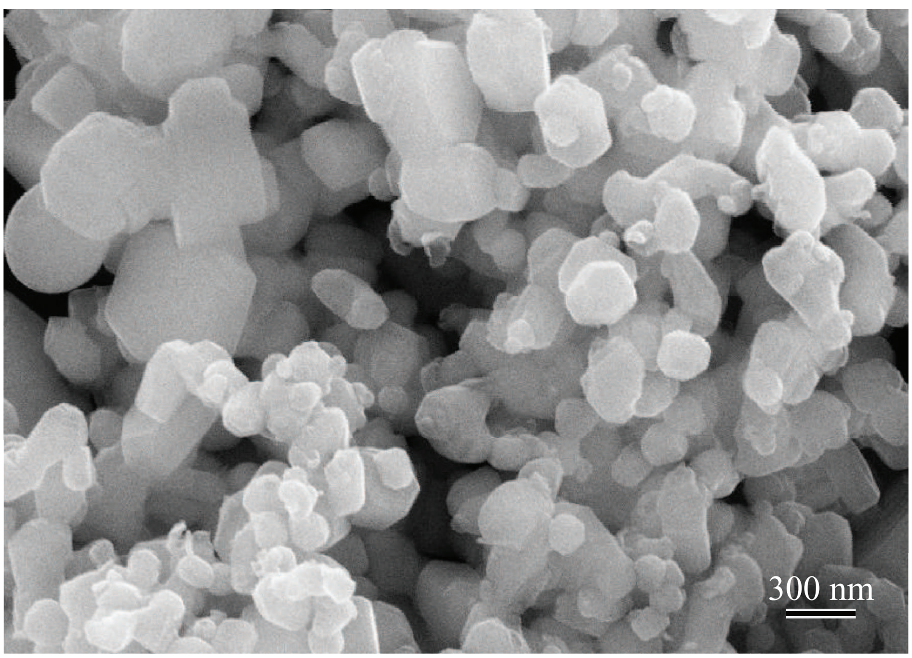

Figure 3: SEM photomicrograph a of ZrB_2 sample heat-treated at 1300°C for 2 h in a graphite tube furnace.

3.0) heat-treated at 1300°C showing nearly-spherical particles of sizes 200-600 nm.

III.1.3 ZrB_2-TaB_2 Sub-micron Powder Mixture

A solid solution of tantalum zirconium oxide ($TaZr_{2.75}O_8$) was detected after heat-treatment at 700°C. This phase was at its highest concentration at 1000°C and was resorbed above 1250°C. TaC was observed after heat-treatments at 1100 and 1150°C. TaC was an intermediate product, which reacted with B_2O_3 at ~1150°C to form TaB_2:

$$2TaC_{(s)} + 4C_{(s)} + 2B_2O_{3(l)} \rightarrow 2TaB_{2(s)} + 6CO_{(g)}$$

ZrB_2 first appeared at 1150°C. There was a significant increase in peak intensity for this phase over the range 1250-1400°C. Between 1400 and 1600°C, ZrB_2 and TaB_2 formed a solid solution as evidenced by the merging of their respective XRD peaks after heat treatment at and above 1600°C.

Weight loss increased abruptly from 1100°C to 1300°C due to carbothermal reduction, as was the case for ZrB_2 alone. This terminated at 1300°C. Figure 4 depicts the microstructure

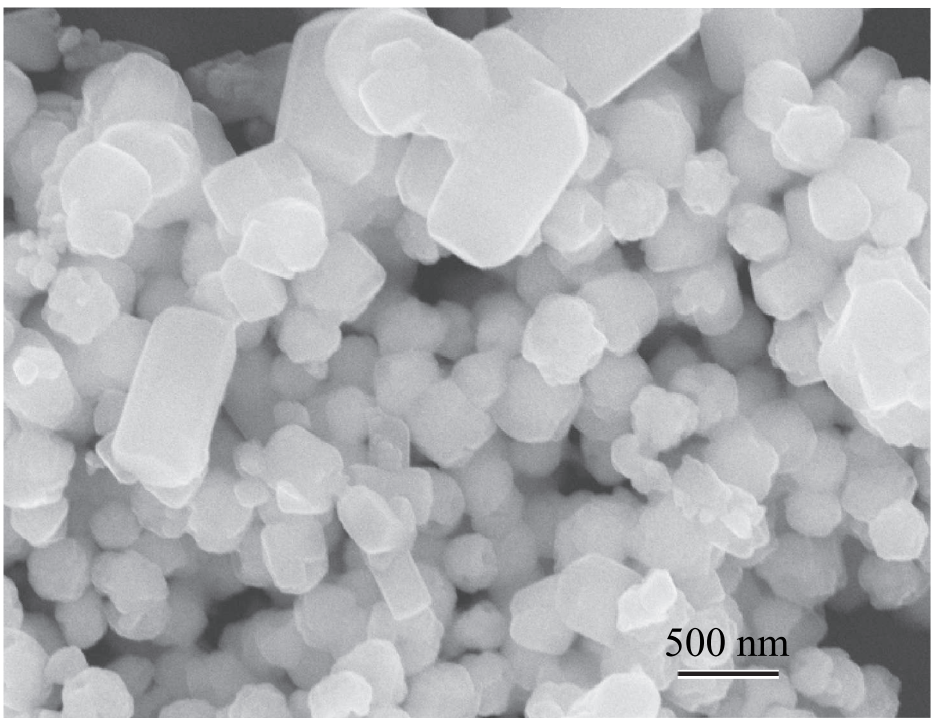

Figure 4: SEM micrograph of ZrB_2-TaB_2 heat-treated at 1300°C for 2 h.

of the ZrB_2-TaB_2 powder heat-treated at 1300°C for 2 h. EDS analysis implies that each particle contained both ZrB_2 and TaB_2. Particle sizes appear in the range of 200-600 nm.

III.2 Oxidation Resistance

Commercially-available powders were used for raw materials. The compositions of synthesized powder mixtures are given in Table 1. These compositions were uniaxially pressed into cylindrical pellets, cold isostatically pressed, sintered in flowing argon at 2000°C, and then hot isostatically pressed (HIPed) at 1800°C. All post-HIPed specimens were at or very near their theoretical densities. Specimens were exposed to flowing dry air in a thermogravimetric analyzer at a constant heating rate of 3°C/min over the range 1150-1550°C.

Figure 5 shows the mass changes for ZrB_2-B_4C with varying concentrations of SiC additions. With SiC additions increasing up to 13.8 vol% SiC (ZBS4), weight gain continuously increased, accelerating over the temperature range of ~1400-1500°C. Slopes of mass change with temperature were the same for all compositions (except ZBS18) up to ~1350°C. This is consistent with the work of others [34, 35] which shows that over this lower temperature range, SiC does not oxidize to contribute to forming a protective layer. For SiC contents of 19.3 vol% and above (ZBS8-ZBS18), temperature spans of mass loss are apparent. In these ranges, the net rate of mass gain from oxidation was less than the rate of mass loss from volatilization of B_2O_3 from the amorphous borosilicate surface layer. At temperatures above these ranges, mass gain resumed, indicating the dominance of accelerating oxygen diffusion through the amorphous silica surface layer.

As shown in Figure 6, for approximately the same SiC content, tantalum additions (in the form of TaB_2) resulted in improved oxidation resistance over the entire evaluated temperature span (1150-1550°C). Figure 7 shows the effect of tantalum additions, both in the form of TaB_2 and $TaSi_2$. Additions of $TaSi_2$ resulted in greater oxidation resistance than TaB_2 additions, though both additives were helpful. This is expected since oxidations of both Ta and Si contribute to protective species—SiO_2 which forms the protective surface glass, and Ta_2O_5 which has been argued to facilitate phase separation (with associated viscosity increase and oxygen diffusivity decrease) in the amorphous layer [40, 42]. This result is even more striking in light of the fact that a significant weight gain should occur from the oxidation of $TaSi_2$.

Figure 8 compares the lowest mass-gain compositions (after heating to 1550°C) of the different categories. SiC addition decreased the rate of mass gain starting at ~1290°C and there was a range mass loss of 1325-1410°C. SiC addition along with combined TaB_2 and $TaSi_2$ additions formed the composition with the lowest mass gain over the entire spectrum

Table 1: Sample Compositions

Code	ZrB_2		B_4C		SiC		TaB_2		$TaSi_2$	
	Vol%	Mol%	Vol%	Mol%	Vol%	Mol%	Vol%	Mol%	Vol%	Mol%
ZB3	90.0	91.4	10.0	8.6	0.0	0.0	0.0	0.0	0.0	0.0
ZB5	86.5	88.3	13.5	11.7	0.0	0.0	0.0	0.0	0.0	0.0
ZBS2	80.4	77.4	8.9	7.2	10.7	15.3	0.0	0.0	0.0	0.0
ZBS4	77.6	73.6	8.6	6.9	13.8	19.5	0.0	0.0	0.0	0.0
ZBS6	75.0	70.2	8.3	6.6	16.7	23.2	0.0	0.0	0.0	0.0
ZBS8	72.6	67.1	8.1	6.3	19.3	26.5	0.0	0.0	0.0	0.0
ZBS10	70.3	64.2	7.8	6.0	21.9	29.7	0.0	0.0	0.0	0.0
ZBS14	64.7	57.5	7.2	5.4	28.1	37.1	0.0	0.0	0.0	0.0
ZBS18	58.8	50.7	6.5	4.7	34.7	44.5	0.0	0.0	0.0	0.0
ZTBS1-1	65.2	59.8	7.3	5.7	20.5	27.9	7.0	6.6	0.0	0.0
ZTBS1-5	64.2	59.8	7.1	5.6	20.2	28.0	3.5	3.4	5.0	3.3
ZTBS1-9	63.3	59.8	7.0	5.6	19.9	28.0	0.0	0.0	9.8	6.6
ZTBS2-1	58.1	53.2	7.3	5.6	20.5	27.9	14.1	13.3	0.0	0.0

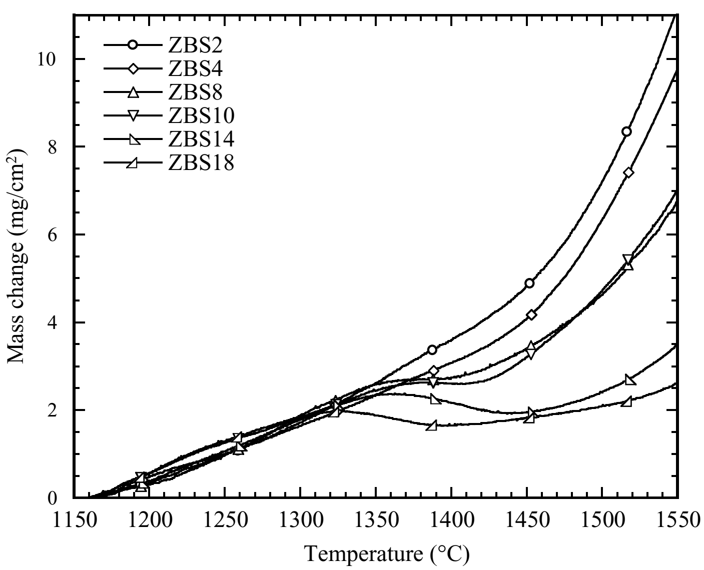

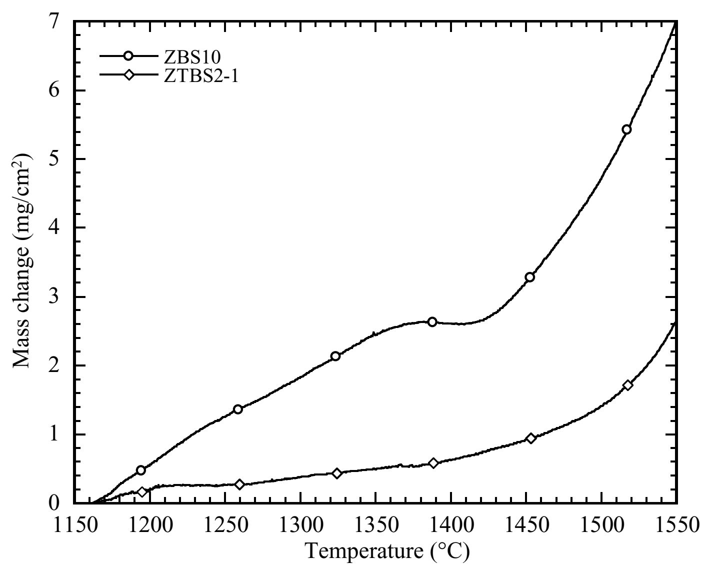

Figure 5: (left) TG of ZrB_2-B_4C specimens with varying amounts of SiC. Volume percentages of SiC increased from 10.7 for ZBS2 to 34.7 for ZBS18.

Figure 6: (right) Effect of substitution of TaB_2 for ZrB_2: ZBS10 contains only ZrB_2. ZTBS2-1 contains a mixture of ZrB_2 and TaB_2. Concentrations of B_4C and SiC were held approximately constant.

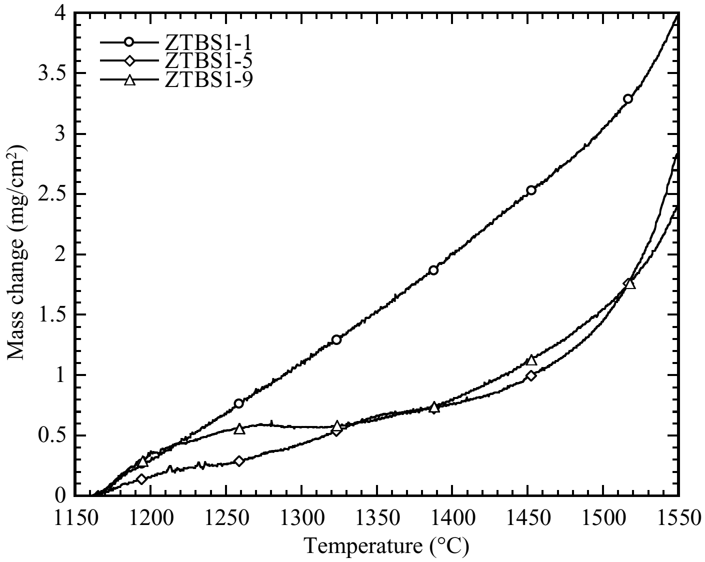

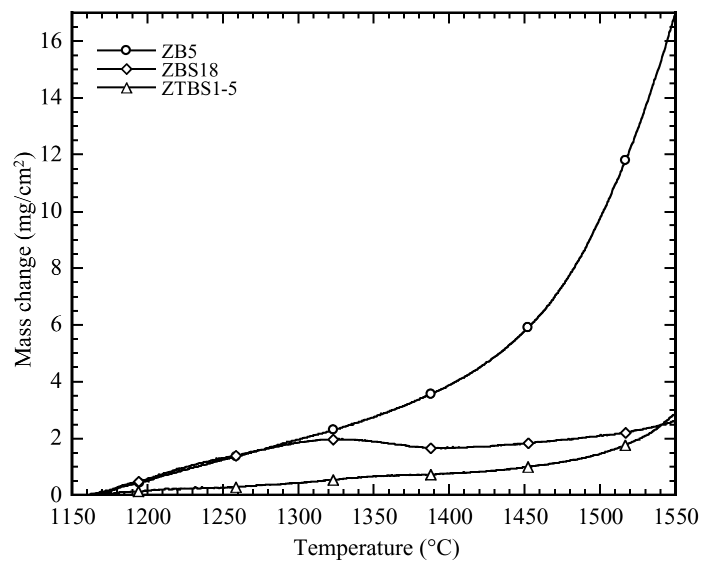

Figure 7: (left) TG of ZrB_2-B_4C-SiC specimens with TaB_2 and $TaSi_2$ additions. ZTBS1-1 has only TaB_2, ZTBS1-9 has only $TaSi_2$, and ZTBS1-5 has both additives.

Figure 8: (right) Comparison of various compositions: ZB5 has no silicon-bearing constituents. ZBS18 contains 34.7 vol% SiC, and ZTBS1-5 contains SiC, TaB_2 and $TaSi_2$.

of evaluated temperatures.

Figure 9 shows three layers in the cross-section of oxidized ZBS18. A 5 μm surface layer with a glassy appearance contained silicon and oxygen, but was devoid of zirconium. A second porous layer of $\sim$20 μm thickness contained Zr, Si, O, and trace carbon. This porosity could have formed via capillary extraction of the silica from oxidized SiC to the amorphous silica surface layer, or from formation of $SiO_{(g)}$ as proposed in other work [37, 38]. Beneath these layers was a well-densified matrix containing Zr, Si, and carbon, but no oxygen. Figure 10 similarly shows three distinct regions in the cross-section of oxidized ZBTS1-1. A $\sim$5 μm glassy surface coating contained silicon, oxygen, and only a trace quantity of zirconium. There was no indication of the presence of tantalum in this layer, but the Ta EDS peak can be masked by the presense of silicon. A second layer of $\sim$20 μm thick contained zirconium, tantalum, silicon, carbon, and oxygen. This region appeared less porous than the corresponding second layer in ZBS18. This may be the result of the Ta_2O_5-SiO_2 liquid phase having a higher viscosity, leaving it less vulnerable to capillary extraction to the amorphous surface layer. This second oxide layer would then likely be more protective of the underlying

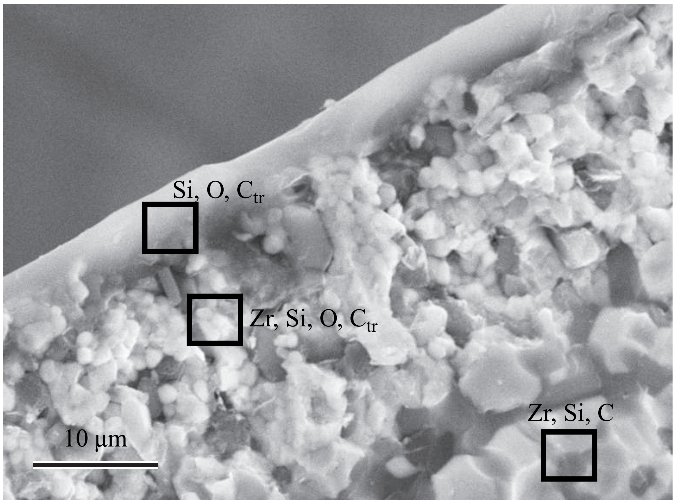

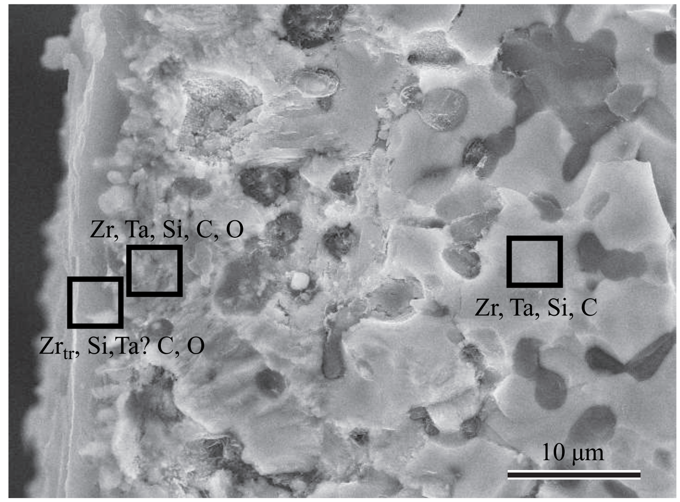

Figure 9: (left) Secondary electron SEM micrograph of ZBS18 (58.8 vol% ZrB_2, 6.5 vol% B_4C, and 34.7 vol% SiC).

Figure 10: (right) Secondary electron SEM micrograph of ZBTS1-1 (65.2 vol% ZrB_2, 7.3 vol% B_4C, 20.5 vol% SiC, and 7.0 vol% TaB_2).

diboride than the analogous layer in the ZBS series. The specimen interior contained Zr, Ta, C, and Si, with no oxygen detected.

References

[1] Y. Murata and E. B. Whitney, "Densification and Wear Resistance of Ceramic Systems: III. Tantalum Mononitride-Zirconium Diboride," *Am. Ceram. Soc. Bull.,* **48** [7] 698-702 (1969).

[2] Y. Murata, "Densification and Wear Resistance of HfN-ZrB_2 Compositions," *Am. Ceram. Soc. Bull.*, **52** [3] 255-259 (1973).

[3] X. Zhang, P. Hu, S. Meng, J. Han, and B. Wang, "Microstructure and Mechanical Properties of ZrB_2-Based Ceramics," *Key Engin. Mater.*, **312** 287-292 (2006).

[4] H. Blumenthal, "Production of Transition Metal Diborides and their Solid Solutions from Metal Oxides and Boron Oxide," *Powder Met. Bull.*, **7** [3-6] 79-81 (1956).

[5] A. I. Karasev, "Preparation of Zirconium Diboride by the Carbothermic Reduction of Mixtures of Zirconium and Boron Oxides," *Poroshkovaya Met.*, **11** [131] 80-84 (1973).

[6] A. W. Weimer, R. P. Roach, C. N. Haney, W. G. Moore, and W. Rafaniello, "Rapid Carbothermal Reduction of Boron Oxide in a Graphite Transport Reactor," *AICHE J.*, **37** [5] 759-768 (1991).

[7] Maeda, T. Yoshikawa, K. Kusakabe, and S. Morooka, "Synthesis of Ultrafine NbB_2 Powder by Rapid Carbothermal Reduction in a Vertical Tubular Reactor," *J. Alloys and Compounds*, **215** 127-134 (1994).

[8] T. Saito, T. Fukuka, H. Maeda, K. Kusakabe, and S. Morooka, "Synthesis of Ultrafine TiB_2 Particles by Rapid Carbothermal Reduction in a Particulate Transport Reactor," *J. Mater. Sci.*, **32** 3933-3938 (1997).

[9] H. Martin, R. Ecke, and E. Muller, "Synthesis of Nanocrystalline Silicon Carbide Powder by Carbothermal Reduction," *J. Eur. Ceram. Soc.*, **18** 1737-1742 (1998).

[10] H. Tanaka and Y. Kurachi, "Synthesis of β-SiC Powder from Organic Precursor and its Sinterability," *Ceram. International*, **14** 109-115 (1988).

[11] D. Huang and Y. Ikuhara, "Characterization of β-Silicon Carbide Powders Synthesized by the Carbothermal Reduction of Silicon Carbide Precursors," *J. Am. Ceram. Soc.*, **81** 3173-3176 (1998).

[12] Y. Sugahara, Y. Takeda, K. Kuroda, and C. Kato, "Carbothermal Reduction Process of Precursors Derived from Alkoxides for Synthesis of Boron-Doped SiC Powder," *J. Mater. Sci. Lett.*, **8** 944-946 (1989).

[13] G. C. Wei, C. R. Kennedy, and L. A. Harris, "Synthesis of Sinterable SiC Powders by Carbothermic Reduction of Gel-Derived Precursors and Pyrolysis of Polycarbosilane," *Am. Ceram. Soc. Bull.*, **63** [8] 1054-1061 (1984).

[14] I. Hasegawa, T. Nakamura, S. Motojima, and M. Kajiwara, "Synthesis of Silicon Carbide Fibers by Sol-Gel Processing," *J. Sol-Gel Sci. Tech.*, **8** 577-579 (1997).

[15] A. W. Weimer, W. G. Moore, R. P. Roach, J. E. Hitt, R. S. Dixit, and S. E. Pratsinis, "Kinetics of Carbothermal Reduction Synthesis of Boron Carbide," *J. Am. Ceram. Soc.*, **75** [9] 2509-2514 (1992).

[16] I. Hasegawa, Y. Fukuda, and M. Kajiwara, "Inorganic-Organic Hybrid Route to Synthesis of ZrC and Si-Zr-C Fibres," *Ceram. Int.*, **25** 523-527 (1999).

[17] Z. Jiang and W.E. Rhine, "Preparation of TiN and TiC from a Polymer Precursor," *Chem. Mater.*, **3** 1132-1137 (1991).

[18] D. R. Stanley, J. D. Birchall, J. N. K. Hyland, L. Thomas, and K. Hodgetts, "Carbothermal Synthesis of Binary (MX) and Ternary (M1,M2,X) Carbides, Nitrides and Borides from Polymeric Precursors," *J. Mater. Chem.*, **2** [2] 149-156 (1992).

[19] H. Preiss, B. Meyer, and C. Olschewski, "Preparation of Molybdenum and Tungsten Carbides from Solution Derived Precursors," *J. Mat. Sci.*, **33** 712-722 (1998).

[20] C. A. Wang, M. D. Sacks, G. A. Staab, and Z. Cheng, "Solution-Based Processing of Nanocrystalline SiC," *Ceram. Eng. Sci. Proc.*, **23** [4] 701-709 (2002).

[21] Z. Cheng, M. D. Sacks, C. Wang, and Z. Yang, "Preparation of Nanocrystalline Silicon Carbide Powders by Carbothermal Reduction," *Ceram. Trans.*, **154** 15-25 (2003).

[22] H. Preiss, E. Schierhorn, K. W. Brzezinka, "Synthesis of Polymeric Titanium and Zirconium Precursors and Preparation of Carbide Fibers and Films," *J. Mater. Sci.*, **33** [19] 4697-4706 (1998).

[23] E. L. Sham, E. M. Farfan-Torres, S. Bruque-Gamez, and J. J. Rodriguez-Jimenez, "Synthesis of ZrC/ZrO_2 by Pyrolysis of Modified Zirconium Alkoxide Precursors," *Solid State Ionics*, **63-65** 45-51 (1993).

[24] C. A. Wang and M. D. Sacks, "Processing of Nanocrystalline Hafnium Carbide Powders," *Ceram. Eng. Sci. Proc.*, **24** [A] 33-40 (2003).

[25] C. A. Wang, M. D. Sacks, and Z. Yang, "Preparation of Nanocrystalline Hafnium Carbide Powders by Carbothermal Reduction," *Ceram. Trans.*, 27-36 (2003).

[26] Z. Hu, M. D. Sacks, G. A. Staab, C. A. Wang, and A. Jain, "Solution-Based Processing of Nanocrystalline ZrC," *Ceram. Eng. Sci. Proc.*, **23** [4] 711-717 (2002).

[27] A. Jain, M. D. Sacks, C. A. Wang, M. Middlemas, and Z. Cheng, "Processing of Nanocrystalline Zirconium Carbide Powders," *Ceram. Eng. Sci. Proc.*, **24**[A] 41-49 (2003).

[28] A. Jain, M. D. Sacks, and C. A. Wang, "Preparation of Nanocrystalline Zirconium Carbide Powders by Carbothermal Reduction," *Ceram. Trans.*, **154** 37-46 (2003).

[29] M. Gash, D. Ellerby, E. Irby, S. Beckman, M. Gusman, and S. Johnson, "Processing, Properties, and Arc Jet Oxidation of Hafnium Diboride/Silicon Carbide Ultra High Temperature Ceramics," *J. Mater. Sci.*, **39** 5925-37 (2004).

[30] D. Sciti, M. Brach, and A. Bellosi, "Oxidation Behavior of a Pressureless Sintered ZrB_2-$MoSi_2$ Ceramic Composite," *J. Mat. Res.*, **20** [4] 922-930 (2005).

[31] W. G. Fahrenholtz, G. E. Hilmas, I. G. Talmy, and J. A. Zaykoski, "Refractory Diborides of Zirconium and Hafnium," *J. Am. Ceram. Soc.*, **90** [5] 1347-1364 (2007).

[32] S. C. Zhang, G. E. Hilmas, and W. G. Fahrenholtz, "Pressureless Densification of Zirconium Diboride with Boron Carbide Additions," *J. Am. Ceram. Soc.*, **89** [5] 1544-1550 (2006).

[33] A. L. Chamberlain, W. G. Fahrenholtz, and G. E. Hilmas, "Pressureless Sintering of Zirconium Diboride," *J. Am. Ceram. Soc.*, **89** [2] 450-56 (2006).

[34] W. C. Tripp, H. H. Davis, and H. C. Graham, "Effect of an SiC Addition on the Oxidation of ZrB_2," *Am. Ceram. Soc. Bull.*, **52** [8] 612-616 (1973).

[35] M. M. Opeka, I. G. Talmy, E. J. Wuchina, J. A. Zaykosi, and S. J. Causey, "Mechanical, Thermal, and Oxidation Properties of Refractory Hafnium and Zirconium Compounds," *J. Eur. Ceram. Soc.*, **19** [12-14] 2405-2414 (1999).

[36] A. Rezaie, W. G. Fahrenholtz, and G. E. Hilmas, "Oxidation of Zirconium Diboride-Silicon Carbide at 1500°C in a Low Partial Pressure of Oxygen, *J. Am. Ceram. Soc.*, **89** [10] 3240-45 (2006).

[37] E. J. Opila, M. C. Halbig, "Oxidation of ZrB_2-SiC," *Ceram. Eng. Sci. Proc.*, **22** [3] 221-228 (2001).

[38] A. Rezaie, W. G. Fahrenholtz, and G. E. Hilmas, "Evolution of Structure During the Oxidation of Zirconium Diboride-Silicon Carbide in Air up to 1500°C," *J. Europ. Ceram. Soc.*, **27** 2495-2501 (2007).

[39] M. Opeka, I. Talmy, J. Zaykoski, "Oxidation-based Materials Selection for 2000°C $^+$ Hypersonic Aerosurfaces: Theoretical Considerations and Historical Experience," *J. Mater. Sci.*, **39** [19] 5887-5904 (2004).

[40] I. G. Talmy, J. A. Zaykoski, M. M. Opeka, S. Dallek, "Oxidation of ZrB_2 Ceramics Modified With SiC and Group IV-VI Transition Metal Diborides," *Elec. Chem. Soc. Proc.*, **12** 144-158 (2001).

[41] W. Vogel, *Glass Chemistry*, 2nd Ed., Springer-Verlag, New York (1994).

[42] E. J. Opila, S. Levine, J. Lorincz, "Oxidation of ZrB_2- and HfB_2-based Ultra-high Temperature Ceramics: Effect of Ta Additions," *J. Mater. Sci.*, **39** [19] 5969-5977 (2004).

[43] I. G. Talmy, J. A. Zaykoski, M. M. Opeka, and A. H. Smith, "Properties of Ceramics in the System ZrB_2-Ta_5Si_3," *J. Mater. Res.,* **21** [10] 2593-99 (2006).

[44] S. R. Levine, E. J. Opila, "Tantalum Addition to Zirconium Diboride for Improved Oxidation Resistance," NASA/TM-2003-212483.

[45] X. Zhang, P. Hu, J. Han, L. Xu, and S. Meng, "The Addition of Lanthanum Hexaboride to Zirconium Diboride for Improved Oxidation Resistance," *Scripta Mater.*, **57** 1036-39 (2007).